

Thermal history of Vesta's crust constrained by U-Pb dating and trace element chemistry of zircon in the Agoult eucrite. T. Iizuka¹, A. Yamaguchi², M. K. Haba², Y. Amelin³, P. Holden³, S. Zink³, M. H. Huyskens³, and T. R. Ireland³, ¹Department of Earth and Planetary Science, The University of Tokyo, Hongo 7-3-1, Bunkyo, Tokyo 113-0033, Japan. ²National Institute of Polar Research, Tachikawa, Tokyo 190-8518, Japan, ³Research School of Earth Sciences, The Australian National University, Canberra ACT, Australia.

Introduction:

Non-cumulate eucrites represent basaltic crust that experienced a complex thermal history involving multistage metamorphism, metasomatism and impact events, probably on asteroid Vesta [e.g., 1-4]. To better constrain the thermal history of these rocks and their parent body, we have integrated high-precision U-Pb age and trace element data for eucrite zircon. Zircon is a common accessory phase in intermediate-felsic igneous rocks and high-grade metamorphic rocks, and single grains of zircon can be precisely dated by the U-Pb chronometer. Due to its robustness zircon can retain primary chemical signatures, which can reveal conditions of crystallization, through post-crystallization processes. These signatures include Ti content in zircon, which is a measure of its crystallization temperature [5], and the magnitude of Ce enrichment relative to neighboring La and Pr, which is a function of the oxidation state [6]. Thus, zircon is a suitable mineral for retrieving the primary chemical features of samples having a complex geologic history. Yet, the rarity and typically very small (<20 μm) crystal size [7,8] has prevented comprehensive study and utilization of eucrite zircon.

We have found that the eucrite Agoult, an unbrecciated eucrite with granulitic textures [9], contains exceptionally large zircon grains with sizes up to 80 μm . These large grains allow us to conduct the first combined high-precision U-Pb dating, Ti-thermometry and Ce-oxybarometry on eucrite zircon. The results place new constraints on the early thermal history of Vesta's crust.

Results:

The zircon in the Agoult meteorite typically occurs in association with ilmenite, spinel, tridymite and/or troilite in the mesostasis (Fig. 1). Back scattered electron and cathodoluminescence imaging show no clear zoning structure in the zircon grains.

Trace element data were obtained *in situ* from eleven separate spots on seven zircon grains using ion microprobe. The Agoult zircons have Ti contents ranging from 37 to 55 ppm. All grains have REE patterns with strong depletion in LREE and prominent negative Eu anomalies, but restricted positive Ce anomalies (Ce/Ce^* value of 1.9 ± 1.7 , 2 s.d. after rejection of one outlier).

High precision U-Pb isotopic dating was carried out using ID-TIMS. The results are plotted on a concordia diagram in Fig. 2. All dated zircon grains

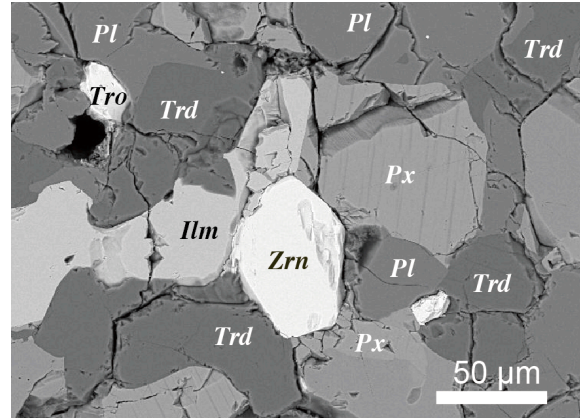


Fig. 1: BSE image showing a zircon grain within the mesostasis of Agoult. Mineral abbreviations are as follow: Ilm, ilmenite; Pl, plagioclase; Px, pyroxene; Trd, tridymite; Tro, troilite; Zrn, zircon.

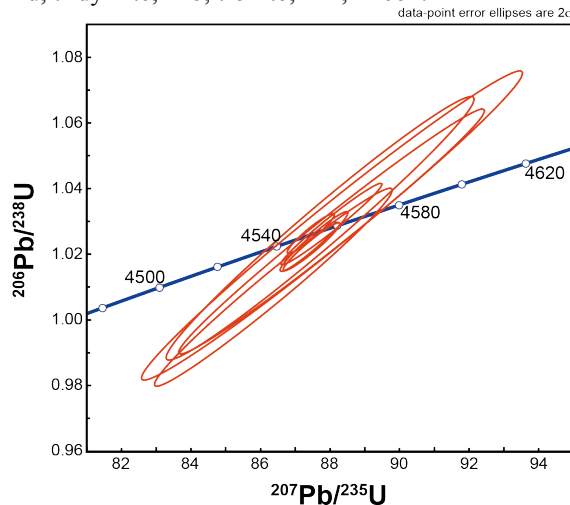


Fig. 2: Concordia plot of U-Pb isotopic data for the Agoult zircon.

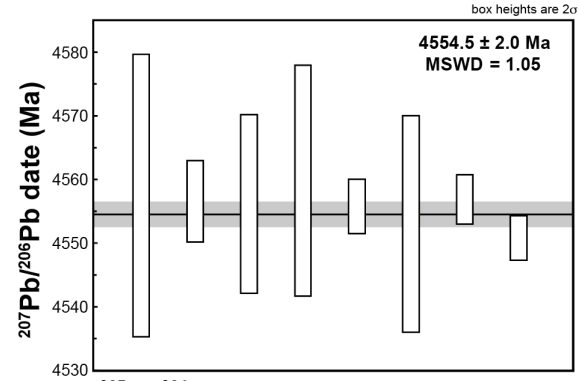


Fig. 3: $^{207}\text{Pb}/^{206}\text{Pb}$ dates and the weighted average (bold line) with 95% confidence interval (shaded area).

have concordant U-Pb systems and identical $^{207}\text{Pb}/^{206}\text{Pb}$ dates within analytical uncertainty. The $^{207}\text{Pb}/^{206}\text{Pb}$ dates yield a weighted average of 4554.5 ± 2.0 Ma (2σ , MSWD = 1.05) using a $^{238}\text{U}/^{235}\text{U}$ of 137.708 ± 0.016 obtained for the Agoult whole-rock fractions [10] (Fig. 3).

Discussion:

All analyzed Agoult zircon grains have identical $^{207}\text{Pb}/^{206}\text{Pb}$ dates with concordant U-Pb systems (Fig. 2), validating that the U-Pb systems are pristine since the crystallization and, therefore, that the weighted average value of the $^{207}\text{Pb}/^{206}\text{Pb}$ dates (4554.5 ± 2.0 Ma) can be interpreted to reflect the time of the zircon crystallization. The Agoult zircon $^{207}\text{Pb}/^{206}\text{Pb}$ age is in good agreement with previously reported but less precise zircon $^{207}\text{Pb}/^{206}\text{Pb}$ ages for most basaltic eucrites [11–13], suggesting ubiquitous zircon growth in basaltic crust on Vesta at that time.

The Ti contents of 37–55 ppm in the Agoult zircon grains correspond crystallization temperatures of 885–935 °C with the average of 905 ± 32 °C (2 s.d.). The estimated temperatures are substantially lower than the eutectic point of eucrite at ca. 1050 °C [14,15] and similar to the equilibration temperatures of pyroxenes in basaltic eucrites [2]. In addition, we find that some ilmenite grains in Agoult contain tiny needles or blobs of baddeleyite, suggesting that the close association of zircon-ilmenite-tridymite results from metamorphic zircon growth through Zr release from ilmenite followed by reaction with tridymite. Thus, we consider the zircon $^{207}\text{Pb}/^{206}\text{Pb}$ age as the timing of the widespread thermal metamorphism in Vesta’s crust that lead to pyroxene equilibration and metamorphic zircon growth.

Given a zircon crystallization temperature, the magnitude of Ce anomaly in the zircon can be used to constrain the oxygen fugacity ($f\text{O}_2$) during the crystallization [6]. The Ce/Ce^* value of 1.9 ± 1.7 combined with the crystallization temperature of 905 ± 32 °C for the Agoult zircon constrains the $f\text{O}_2$ to below that of the iron-wüstite (IW) buffer (Fig. 4).

The basaltic magmatism on Vesta is considered to proceed at a $f\text{O}_2$ of one log unit below the IW buffer (IW -1) based on the liquidus mineral assemblages and major element compositions of basaltic eucrites [14,16]. By contrast, analyses of Cr-spinels in fluid-metasomatic veins in the eucrite NWA 5738 indicate their crystallization at a $f\text{O}_2$ of IW +3 [17]. The new constraint on the $f\text{O}_2$ during Agoult zircon crystallization suggests that basaltic crust had remained under reducing conditions during the high-temperature metamorphism at 4554 Ma, likely due to the absence of oxidizing agents such as aqueous fluid at that time.

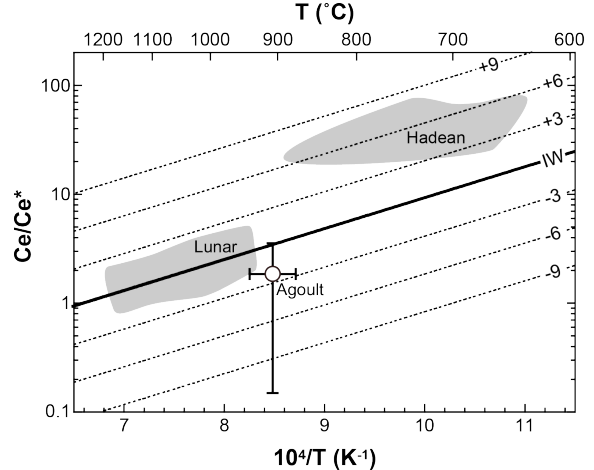


Fig. 4: Plot of Ce/Ce^* versus $1/T$ for zircons from the Agoult eucrite, with experimentally calibrated oxygen fugacity curves relative to the iron-wustite (IW) buffer (after [6]). Shaded areas show the fields of lunar zircons [18] and Hadean terrestrial zircons with $\delta^{18}\text{O}$ in the mantle equilibrium range [19–21]. The Agoult zircon data indicate its crystallization at a $f\text{O}_2$ below than the IW buffer.

References:

- [1] Takeda H. and Graham A. L. (1991) *Meteoritics*, 26, 129–134.
- [2] Yamaguchi A. et al. (1996) *Icarus*, 124, 97–112.
- [3] Bogard D. D. and Garrison D. H. (2003) *Meteorit. Planet. Sci.*, 38, 669–710.
- [4] Barrat J. A et al. (2011) *Geochim. Cosmochim. Acta*, 75, 3839–3852.
- [5] Watson E. B. and Harrison T. M. (2005) *Science*, 308, 841–844.
- [6] Trail D. et al. (2011) *Nature*, 480, 79–82.
- [7] Haba M. K. et al. (2014) *Earth Planet. Sci. Lett.*, 387, 10–21.
- [8] Roszjar J. et al. (2014) *Chemie der Erde*, 74, 453–469.
- [9] Yamaguchi A. et al. (2009) *Geochim. Cosmochim. Acta*, 73, 7162–7182.
- [10] Kaltenbach A. (2013) PhD Thesis, Univ. Otago.
- [11] Ireland T. R. and Bukovanska M. (2003) *Geochim. Cosmochim. Acta*, 67, 4849–4856.
- [12] Misawa K. (2005) *Geochim. Cosmochim. Acta*, 69, 5847–5861.
- [13] Zhou et al. (2013) *Geochim. Cosmochim. Acta*, 110, 152–175.
- [14] Stolper E. (1977) *Geochim. Cosmochim. Acta*, 41, 587–611.
- [15] Yamaguchi A. et al. (2013) *Earth Planet. Sci. Lett.*, 368, 101–109.
- [16] Jurewicz A. J. G. et al. (1993) *Geochim. Cosmochim. Acta*, 57, 2123–2139.
- [17] Warren P. H. et al. (2014) *Geochim. Cosmochim. Acta*, 141, 199–227.
- [18] Taylor D. J. et al. (2009) *Earth Planet. Sci. Lett.*, 279, 157–164.
- [19] Cavosie A. J. et al. (2005) *Earth Planet. Sci. Lett.*, 235, 663–681
- [20] Cavosie A. J. et al. (2006) *Geochim. Cosmochim. Acta*, 70, 5601–5616.
- [21] Fu B. et al. (2008) *Contrib. Mineral. Petrol.*, 156, 197–215.